Micromechanical bending of single collagen fibrils using atomic force microscopy

Lanti Yang,[1] Kees O. van der Werf,[2] Bart F.J.M. Koopman,[3] Vinod Subramaniam,[2] Martin L. Bennink,[2] Pieter J. Dijkstra,[1] Jan Feijen[1]

[1]*Polymer Chemistry and Biomaterials, Faculty of Science and Technology and Institute of Biomedical Technology (BMTI), University of Twente, P.O. Box 217, 7500 AE Enschede, The Netherlands*

[2]*Biophysical Engineering, Faculty of Science and Technology and MESA+ Institute for Nanotechnology, University of Twente, P.O. Box 217, 7500 AE Enschede, The Netherlands*

[3]*Biomechanical Engineering, Faculty of Engineering Technology, University of Twente, P.O. Box 217, 7500 AE Enschede, The Netherlands*

Received 16 February 2006; revised 21 July 2006; accepted 19 September 2006
Published online 31 January 2007 in Wiley InterScience (www.interscience.wiley.com). DOI: 10.1002/jbm.a.31127

Abstract: A new micromechanical technique was developed to study the mechanical properties of single collagen fibrils. Single collagen fibrils, the basic components of the collagen fiber, have a characteristic highly organized structure. Fibrils were isolated from collagenous materials and their mechanical properties were studied with atomic force microscopy (AFM). In this study, we determined the Young's modulus of single collagen fibrils at ambient conditions from bending tests after depositing the fibrils on a poly(dimethyl siloxane) (PDMS) substrate containing micro-channels. Force-indentation relationships of freely suspended collagen fibrils were determined by loading them with a tip-less cantilever. From the deflection-piezo displacement curve, force-indentation curves could be deduced. With the assumption that the behavior of collagen fibrils can be described by the linear elastic theory of isotropic materials and that the fibrils are freely supported at the rims, a Young's modulus of 5.4 ± 1.2 GPa was determined. After cross-linking with glutaraldehyde, the Young's modulus of a single fibril increases to 14.7 ± 2.7 GPa. When it is assumed that the fibril would be fixed at the ends of the channel the Young's moduli of native and cross-linked collagen fibrils are calculated to be 1.4 ± 0.3 GPa and 3.8 ± 0.8 GPa, respectively. The minimum and maximum values determined for native and glutaraldehyde cross-linked collagen fibrils represent the boundaries of the Young's modulus. © 2007 Wiley Periodicals, Inc. J Biomed Mater Res 82A: 160–168, 2007

Key words: single collagen fibril; atomic force microscopy; bending test; cross-linking; Young's modulus

INTRODUCTION

Collagen is the principal, tensile stress-bearing component of connective tissue. Over the past decade, several studies have been directed toward the elucidation of the substructures present in collagen to relate the structure to its function and mechanical properties.[1–5] In summary, the hierarchical structure can be described as follows: five tropocollagen molecules (collagen triple helices from which the propeptides are enzymatically removed) assemble into microfibrils. These microfibrils aggregate in the lateral and longitudinal direction to form fibrils.[6–9] The collagen fibrils have a diameter between 10 and 500 nm and further assemble into fibers. It must be noted that microfibrils have never been isolated but researchers nowadays agree on this microfibrillar structure based mainly on X-ray data,[10] three-dimensional imaging using automated electron tomography[11] and atomic force microscopy (AFM) imaging.[12,13]

The macro-mechanical properties of collagenous materials were studied extensively in the past decades. Because of the hierarchical structure of collagen material, the contribution of the different organizational levels to the mechanical behavior appears complicated. With macro-tensile testing, the data presented in the literature on the modulus of elasticity (Young's modulus) of dry collagen tissue and collagen fibers range from 1 to 8 GPa.[14–17] Based on X-ray diffraction studies, Puxkandl et al. reported that the overall strain of the tendon was always larger than the strain in the individual fibrils.[18] In addition,

Correspondence to: J. Feijen; e-mail: J.Feijen@utwente.nl
Contract grant sponsor: ZonMw (Softlink Program); contract grant number: 01SL056

Sasaki and Odajima[19,20] reported different values of Young's modulus by testing collagen molecules, fibrils and tendons. It was found that intermolecular cross-links have a great influence on the mechanical behavior of collagen.

Recently, some studies on the micro-mechanical properties of collagen fibrils and molecules using micromanipulation techniques such as AFM and optical tweezers have been reported.[21–25] Thompson et al. used an AFM to perform pulling experiments on collagen molecules exposed on the surface of a polished bone. They reported that there are "sacrificial bonds" within and between collagen molecules. The force versus extension curves show that these sacrificial bonds can be broken, and prevent the force increasing to a value that may break the collagen backbone. The time needed for these sacrificial bonds to reform after pulling correlates with the time needed for bone to recover its toughness.[21] Later in 2003, Gutsmann et al. in the same group[23] investigated the correlation between periodic patterns in the topography of tendon collagen fibrils and the force-extension curves observed in the force spectroscopy measurements on the sub-units of collagen fibers. They found two different periodic rupture events with a periodicity of 78 and 22 nm. The periodic rupture found by force spectroscopy was consistent with their previous results on the 65 nm D-period and small 23-nm spacing of collagen fibrils.[26] Very recently, Graham et al.[24] measured the force-elongation profiles of single collagen fibrils to investigate the structural changes in single fibrils during elongation. They concluded that the major reorganization of the collagen fibril structure occurs in the 1.5–4.5 nN range. Sun et al.[27] studied the flexibility of individual type I procollagen by stretching the procollagen using optical tweezers. The persistence length, which relates to the flexibility of the collagen molecule, was determined to be 14.5 nm and the contour length to be 309 nm. Comparable results were obtained by Bozec and Horton with an AFM topological and force spectroscopy study on single collagen molecules. They found that the contour length of single collagen molecules is 287 ± 35 nm.[25]

Besides the tensile tests as described above, bending tests form another method to determine the mechanical properties of a specimen.[28,29] In this paper we describe for the first time the use of an atomic force microscope for bending measurements of collagen fibrils that freely span the micro-channels in a polymeric substrate. The force needed to bend a suspended fibril at the center point was determined and fitted to elasticity models to deduce the Young's modulus of a collagen fibril. Similar experiments were performed on collagen fibrils cross-linked with glutaraldehyde, a commonly used cross-linking agent to increase the stability of collagen-based biomaterials.[30,31] The results are discussed in relation to the collagen mechanical properties and its hierarchical structure.

EXPERIMENTAL

Preparation of PDMS substrates

Poly(dimethyl siloxane) (PDMS) molds were prepared using Sylgard 184 silicone elastomer (Dow Corning, Wiesbaden, Germany). The prepolymer was mixed with the curing agent in a 10:1 weight ratio as specified by the manufacturer. After 10 min stirring and 40 min degassing in a vacuum oven, the mixture was poured onto a prepatterned silicon wafer with parallel channels and cured at 70°C overnight. The width and depth of the channels on the prepatterned silicon wafer were ~5 and 1 μm, respectively. After curing, the PDMS layer was peeled off the silicon wafer. The width and depth of the channels in the PDMS were determined by ~10 AFM measurements.

Deposition of collagen fibrils

Bovine Achilles tendon collagen type I from Sigma-Aldrich (Steinheim, Germany) was swollen in hydrochloric acid (0.01*M*) overnight at 0°C. The resulting slurry was shredded for 10 min at 9500 rpm using a Braun MR 500 HC blender (Braun, Kronberg, Germany). The temperature was kept below 5°C. The resulting mixture was filtered using a 74 μm filter (Bellco Glass, collector screen 200 mesh, Vineland, NJ). The helical content of the collagen suspension after filtration was determined by FTIR (Biorad, FTS-60) according to a method described by Friess and Lee.[32] To 1 mL of the filtrate, mainly containing collagen fibrils, 150 mL of PBS (pH = 7.4) was added. Deposition of the collagen fibrils on the PDMS substrates was done by incubating the substrates for 10 min in the diluted fibril dispersion. Subsequently, the collagen deposited PDMS substrates were washed with PBS for 10 min and three times for 10 min each with demineralized water and finally dried under ambient conditions for at least 24 h. Cross-linked collagen fibrils were prepared by mixing 1 mL of the nondiluted fibrillar dispersion with 5 mL of a 10 wt % glutaraldehyde solution and 195 mL phosphate buffer (pH 7.4) for 2 h. The resulting cross-linked fibrils were deposited on the PDMS substrates as described above.

Single collagen fibrils deposited on the PDMS surface were imaged by tapping mode AFM (custom-built instrument) and SEM (LEO Gemini 1550 FEG-SEM). The characteristic D-period of the fibril was characterized by TEM (Philips CM30 Twin/STEM).

Denaturation temperature and free amino group content

The diluted fibril dispersion was centrifuged for 15 min at 4500 rpm (Hettich Mikco Rapid/k, Depex, De Bilt, the Netherlands). The solution was removed and the collagen was washed with MilliQ water twice for 30 min each. Similarly, the diluted cross-linked collagen fibril dispersion was centrifuged as described above and then washed

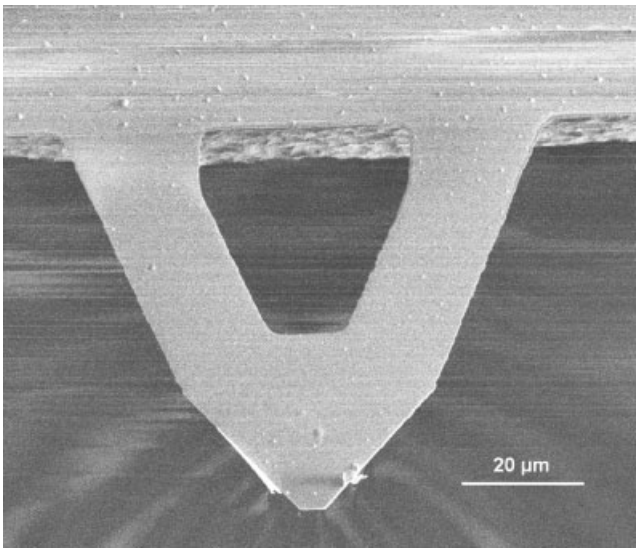

Figure 1. SEM image of an AFM cantilever from which the tip has been removed by FIB.

twice with 4*M* NaCl for 30 min each and four times with MilliQ water for 30 min each.

After the washing steps, both native and cross-linked collagen samples were frozen in liquid nitrogen and subsequently freeze-dried for 24 h.

The degree of cross-linking of the collagen fibrils is related to the increase of the denaturation (shrinkage) temperature (T_d) after cross-linking. The T_d values were determined by means of DSC (DSC 7, Perkin Elmer, Norwalk, CT). Freeze-dried native and cross-linked collagen fibril samples of 3–5 mg were swollen in 50 μL of PBS (pH = 7.4) in high-pressure pans overnight. Samples were heated from 20 to 90°C at a heating rate of 5°C/min. A sample containing 50 μL of PBS (pH = 7.4) was used as a reference. The onset of the endothermic peak was recorded as the T_d.

The free amino group content of native and cross-linked samples was determined using the 2,4,6-trinitrobenzenesulfonic acid (TNBS) assay. Collagen fibril samples of 3–5 mg were incubated for 30 min in 1 mL of a 4 wt % solution of $NaHCO_3$. To this mixture 1 mL of a freshly prepared solution of TNBS (0.5 wt %) in 4 wt % $NaHCO_3$ was added. The resulting mixture was left for 2 h at 40°C. After the addition of HCl (3 mL, 6*M*), the temperature was raised to 60°C. Solubilization of collagen was achieved within 90 min. The resulting solution was diluted with 5.0 mL MilliQ water and cooled to room temperature. The absorbance at 420 nm was measured using a Varian Cary 300 Bio spectrophotometer. A blank was prepared applying the same procedure, except that HCl was added before the addition of TNBS. The absorbance was correlated to the concentration of free amino groups using a calibration curve obtained with glycine. The free amino group content was expressed as the number of free amino groups per 1000 amino acids (n/1000).

Single collagen fibril bending tests

A custom-built AFM combined with an optical microscope was used for the bending tests. Bending experiments were performed using modified triangular silicon nitride cantilevers (coated sharp microlevers MSCT-AUHW, type F, spring constant $k = 0.5$ N/m, Veeco, Cambridge, UK). The tip on the AFM cantilever was removed using focused ion beam (FIB) (FEI, NOVALAB 600 dual beam machine) to prevent damaging of the collagen fibril surface during the bending tests. Also, the width of the cantilever is wider than the fibril diameter, which facilitates the positioning of the cantilever above the fibril. After cutting, the modified cantilevers (Fig. 1) were inspected using the built-in SEM. The spring constant of each tipless cantilever was calibrated by pushing on a precalibrated cantilever as described elsewhere.[33,34]

The sensitivity (*S*) of the applied method, that is the ratio between the bending of the cantilever and the deflection as measured by the quadrant detector, was derived from the force-displacement curve measured on a glass surface. During bending tests, the strain rate in the fibril direction is 0.4 ± 0.1 μm/s with an AFM piezo displacement of 1.5 μm and a frequency of 10 Hz was applied. At different positions on the PDMS surface and on the collagen fibrils (Fig. 2), bending experiments using the AFM cantilever afforded deflection versus piezo displacement curves. From the results force-indentation curves were derived. At least three deflection versus piezo displacement curves were recorded at every position.

RESULTS AND DISCUSSION

Collagen fibril deposition

For the mechanical tests an experimental set-up was prepared consisting of a PDMS surface containing micro channels. The rims of the channels support deposited collagen fibrils and thus allow bending experiments by pushing with an AFM cantilever. AFM measurements of the prepared PDMS sub-

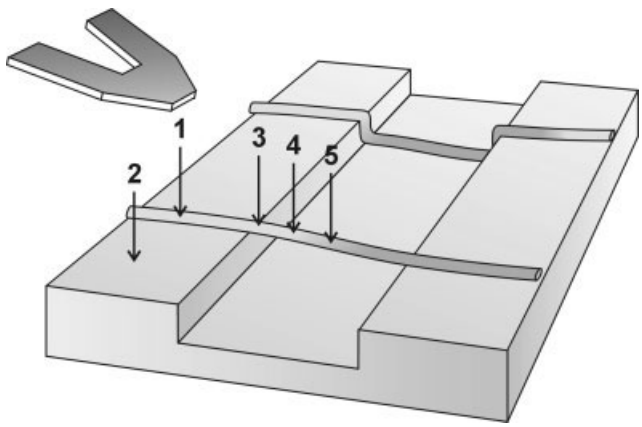

Figure 2. Schematic drawing of collagen fibrils crossing the micrometer-sized channel in PDMS and locations where deflection versus piezo displacement curves were obtained. (1) Collagen fibril on PDMS surface, (2) PDMS surface, (3) fibril at the edge of the channel, (4) fibril between the edge and middle point of the channel, (5) fibril at the middle point of the channel.

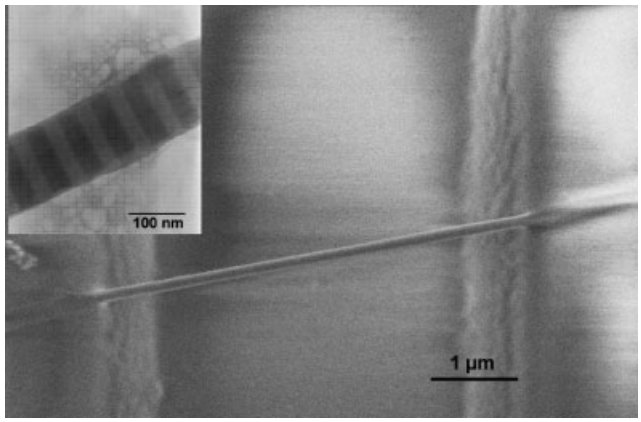

Figure 3. SEM image of a single collagen fibril spanning a channel. Insert: TEM image showing the characteristic D-period of the fibril.

strates showed that the width and depth of the channels are 5 ± 1 μm and 0.7 ± 0.3 μm, respectively. Because of the transparency of the PDMS, the top surface can be imaged using an inverted optical microscope positioned below the sample plate. In this way the position of the AFM cantilever and collagen fibrils deposited on top of the surface can be visualized simultaneously.

Type I collagen fibrils were conveniently obtained through homogenization and filtering bovine Achilles tendon in diluted acetic acid. The helical content of the collagen in the fibrillar suspension was determined with FTIR and revealed a maximum percentage of helicity.[32] The filtrate, a dispersion of fibrils, was subsequently highly diluted. Incubating the PDMS substrate in the diluted dispersion afforded many free single fibrils not interacting with other fibrils on the surface. Both SEM (Fig. 3) and AFM images showed that the diameter of fibrils ranged from ~200 to ~350 nm and the length of the fibril ranged from ~20 to ~200 μm. The characteristic D-period of a single collagen fibril was visualized by TEM (inserted image in Fig. 3) and phase imaging using tapping mode AFM. The visualized D-period ensures that the bending tests (vide supra) were performed on intact single collagen fibrils. Moreover, the denaturation temperature (T_d) and the number of free amino groups (n/1000) of the native and cross-linked collagen fibrils were determined. The T_d of the native fibrils was 57°C and increased to 76°C after cross-linking with glutaraldehyde. The free amino group content of the native collagen fibrils of 28 per 1000 amino acids decreased to a value of eight after crosslinking, which is in line with previous reported data.[31]

Tapping mode AFM revealed that the collagen fibrils were deposited in either of two ways [Fig. 4(A,B)]. Figure 4(A) shows that above the channel the collagen fibril appears thicker when compared to the fibril on the PDMS surface. This is most probably due to the interaction of the AFM tip with the freely suspended part of the collagen fibril. In Figure 4(B), it is shown that the height of the collagen fibril on the channel is much lower than the other parts of the fibril, which indicated that the collagen fibril was

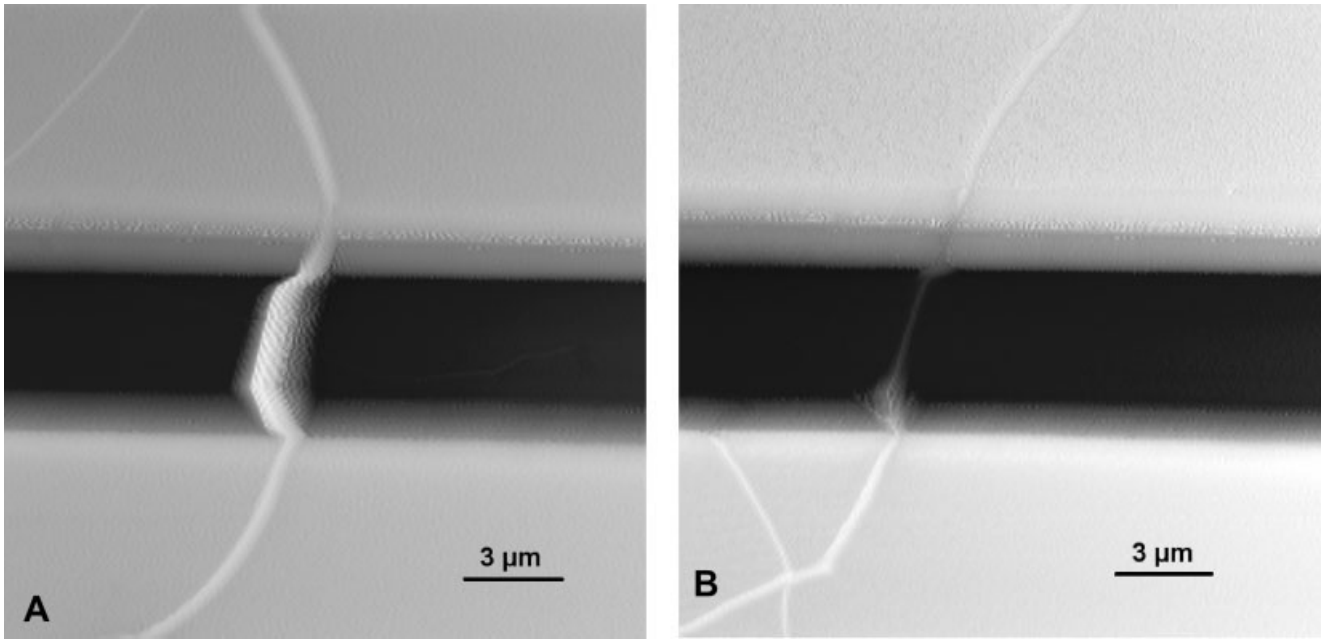

Figure 4. Tapping mode AFM image of two types of collagen fibrils deposition on a PDMS surface with micro channels. The scan size of both images is 20 × 20 μm and the scan direction is from left to right in both images. The z-scale is 2.2 μm for (A) and 1.6 μm for (B). A: Collagen fibril spanning a channel. B: Collagen fibril attached to the bottom of a channel.

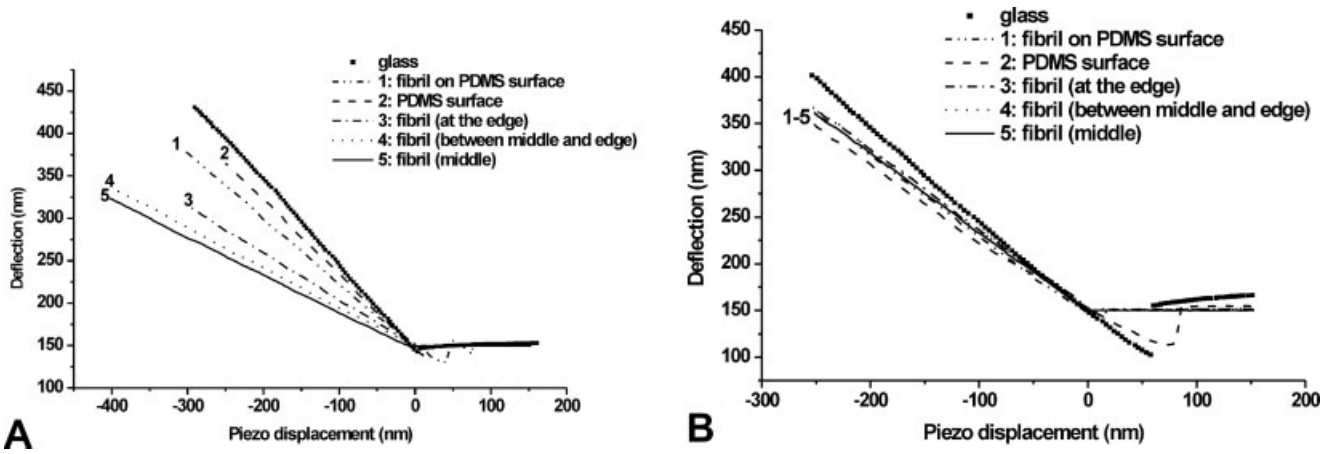

Figure 5. Two examples of deflection–piezo displacement curves of bending tests on different points of the surface; (A) Collagen fibril spanning the channel (B) Collagen fibril attached to the bottom of the channel. The numbers on the curves indicate different bending positions as shown in Figure 2.

attached to the rims and bottom of the channel. Only collagen fibrils with a minimum length of 50 μm and spanning multiple channels were used for bending experiments.

Bending tests

Collagen fibrils spanning the channels were bent with a tip-less cantilever along the fibrils axis. The deflection-piezo displacement curves obtained from these bending tests on different points at the PDMS surface and collagen fibrils as indicated in Figure 2 are shown in Figure 5(A). In the experiments, no difference was found in the deflection-piezo displacement curves after bending the same position three times, which ensures the reproducibility of the test and that no permanent deformation of the collagen fibril occurred. As a reference material and for calibration, deflection-piezo displacement curves on a glass surface were recorded. Because of its high stiffness a large slope was found. Mechanical tests on the PDMS surface and on the fibril supported by the PDMS also showed a large slope. Moving to the center point of the fibril above the channel, the slope of the curve resulting from bending of the fibril decreases. The smallest slope of the deflection-piezo displacement curves was found at the centre point above the channel. As a control the same measurement was performed on a collagen fibril adhered at the rims and bottom of the channel. In this case all curves showed an almost similar slope [Fig. 5(B)]. The mechanical properties of a collagen fibril were derived from the deflection-piezo displacement curve at the center of the fibril above the channel.

Every measured point of the approaching part of the deflection versus piezo displacement curve was used for calculating a force-indentation curve. The force (F) and the indentation (x) in the z-direction were calculated using the following equations:

$$x = A - D \times S \tag{1}$$

$$F = D \times S \times k \tag{2}$$

in which A is the piezo displacement in the z-direction, D is the deflection measured (in Volts), S is the sensitivity of the cantilever and k is the calibrated spring constant of the cantilever. A linear relationship between the force and the indentation for bending the collagen fibril at different positions above the channel is found (Fig. 6).

Following the same procedure as described above, bending tests were also performed using collagen fibrils cross-linked with glutaraldehyde. The gradient of the force-indentation curve on bending the colla-

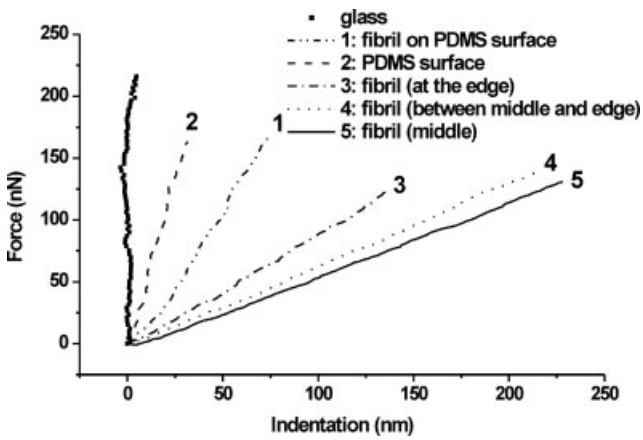

Figure 6. A typical example of a set of force-indentation curves derived from the deflection-piezo displacement curves. The numbers on the curves indicate different bending positions as shown in Figure 2.

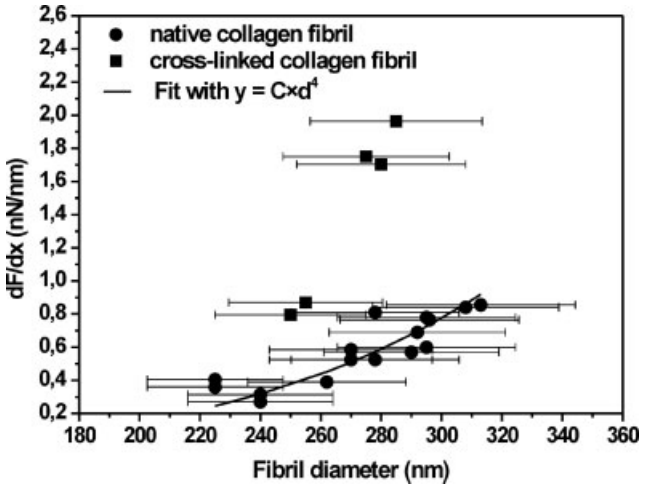

Figure 7. The slope of the force-indentation curve (dF/dx) obtained in different experiments on collagen fibrils as a function of the diameter of the fibril. Filled dots are results from experiments performed on native collagen fibrils. Filled squares are derived from experiments on cross-linked fibrils. dF/dx of native collagen fibrils were fitted with $C \times d^4$, d is the diameter of the fibril and C is a constant. The error bars in the figure are derived from the accuracy of SEM measurements of the diameter of each testing fibril.

gen fibril at its middle point (dF/dx) was obtained in the same way. After every experiment, the radius of the collagen fibril was measured by SEM. In Figure 7, every point represents the results of a single bending test. Because one collagen fibril which can be 100 μm in length can span more than one channel with a width of 5 μm, bending tests were also performed with the same fibril on different channels. The values of dF/dx for the same fibril are similar which illustrates the reproducibility of the tests. Also, some overlapping fibrils were found from high resolution SEM measurements. The gradient of force-indentation for the overlapping fibrils was not included in the results. The results revealed that single collagen fibrils become stiffer after cross-linking with glutaraldehyde.

However, applying a force on the fibril may cause a deformation of the PDMS at the supporting edges which would obscure the results. Using the force-indentation curves, the indentation of the PDMS substrate resulting from the bending of a collagen fibril was estimated. As shown in Figure 8, the largest force upon bending collagen fibrils is ~120 nN at a displacement of the fibril of ~200 nm. As schematically shown in Figure 8(A), the force on the fibril at the end of channel is ~60 nN in a vertical direction. According to the force-indentation curve of the PDMS surface as shown in Figure 6 line 2, the maximum deformation of the PDMS can be estimated to be about 10 nm in the bending direction at a loading force of 60 nN. The deformation of the PDMS surface thus appears only 5% of the indentation of the collagen fibril at the center point, which is regarded negligible.

The gradient (dF/dx) of the force-indentation curve was used to calculate the Young's modulus. Because of the high length to diameter ratio of the

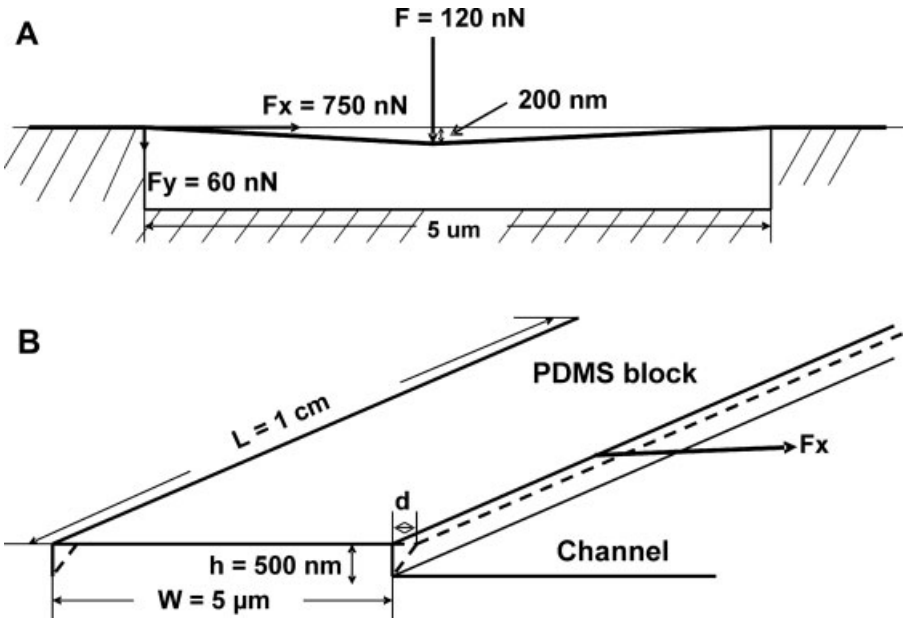

Figure 8. A: Maximum forces on the centre of a collagen fibril and on the PDMS surface during bending. F: the maximum force applied at the center of the collagen fibril with 200 nm indentation; F_x: the force on the fibril at the end of the channel in horizontal direction; F_y: the force on the fibril at the end of the channel in vertical direction (B) The dimensions of the PDMS block and deformation in horizontal direction. L: the length of the PDMS block; w: the width of the PDMS block; h: the height of the channel; d: deformation in the horizontal direction.

collagen fibril and the fact that the force is applied perpendicular to the fibril axis, it is assumed that the mechanical properties of the collagen fibrils can be described by the linear elastic theory of isotropic materials. The Young's modulus of a single collagen fibril can be calculated from the measured force on the middle point of the collagen fibril spanning a channel (Fig. 2) using the expressions[35]:

$$E = \frac{l^3}{48I} \times \frac{\mathrm{dF}}{\mathrm{dx}} \tag{3}$$

$$E = \frac{l^3}{192I} \times \frac{\mathrm{dF}}{\mathrm{dx}} \tag{4}$$

in which I is the moment of inertia and is equal to $1/4\pi R^4$ (the fibril is considered a rod with a circular cross-section with radius R), l is the length of the collagen fibril spanning the channel and dF/dx is the slope of the force-indentation curve obtained from bending the middle point of the collagen fibrils.

Equation 3 represents the condition that the fibril is freely supported by the two ends of the channel. However, because collagen is well known for its surface adhesive properties, the fibril is expected to be strongly adhered to the PDMS and then Eq. (4) has to be used. The Young's modulus of the collagen fibril is calculated from Eqs. (3) and (4) to set the maximum and minimum values of the Young's modulus.

The Young's modulus of single native collagen fibrils was calculated and the results are summarized in Figure 9. The absolute error in the Young's modulus of every individual fibril is derived from the fibril diameter (SEM measurements), the accuracy in determining the length of the channel and the error in determining the spring constant of the cantilever. Because of the high linearity of the force-indentation curves, the error in the linear fit is ignorable. Based on the measurements of native fibrils, the Young's moduli are constant at the measured fibril diameter range. An average Young's modulus of 5.4 ± 1.2 GPa from Eq. (3) and 1.4 ± 0.3 GPa from Eq. (4) were obtained from the bending tests. Because the two models represent extremely different supporting conditions, the real Young's modulus determined from our tests should fit within the range of these two values. The Young's moduli are comparable to those of dry collagen (1–8 GPa) presented in literature.[14–17] After cross-linking with glutaraldehyde, an average Young's modulus value of 14.7 ± 2.7 GPa from Eq. (3) or 3.8 ± 0.8 GPa from Eq. (4) was obtained. Reaction of free amine groups in the collagen with glutaraldehyde results in the formation of different type of cross-links. Most characteristic is the occurrence of short or longer chain cross-links through the possibility of generated intermediates to further polymerize. This will result in bridging collagen molecules as well as microfibrils in the collagen fibril. The increase in the stiffness of collagenous materials on the macro-level is regarded as a result of restriction of the viscous sliding of collagen molecules and fibrils with respect to each other.[36] Here, the increase of the Young's modulus compared to noncrosslinked collagen fibrils is also detected within the single collagen fibril and is ascribed to the reduced possibility of slippage of collagen molecules or segments like microfibrils. However, the Young's modulus of cross-linked fibrils seems to increase with an increase in the fibril diameter. One possible reason is that cross-linking not takes place homogenously within the fibril. Further investigation is needed to determine the distribution of crosslinks and its relation to the fibril mechanical properties.

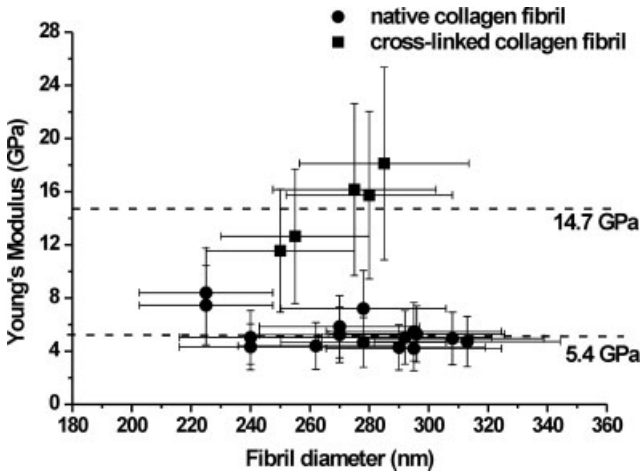

Figure 9. Young's modulus of fibrils with different diameters calculated with the model assuming the fibril is simply supported at the ends of the channel. Filled dots are results from experiments performed on native collagen fibrils. Filled squares are derived from experiments on cross-linked fibrils. (Young's modulus calculated with the model assuming the fibril is fixed at the ends of the channel was [1/4] of the corresponding values presented in the figure.) The absolute error in the Young's modulus of every individual fibril is derived from the fibril diameter (SEM measurements), the accuracy in determining the length of the channel and the error in determining the spring constant of the cantilever.

Using an average value of the Young's modulus of 2.0 ± 0.2 MPa as determined by tensile testing and a shear modulus of PDMS of 0.67 ± 0.07 MPa from literature[37] the maximum deformation of PDMS in a horizontal direction was calculated to be 0.7×10^{-12} m assuming the shear force is distributed along the whole PDMS block. As shown in Figure 8(B), the dimensions of the PDMS block are much larger than the collagen fibril. Therefore, the deformation in the horizontal direction of the PDMS block, which is in the order of 10^{-12} m, can be ignored compared with

the indentation of the collagen fibril (2×10^{-7} m). It has been reported in the literature that the movement of the supporting points or load point during the bending tests would result in a nonlinear force-indentation relationship.[28,38] This nonlinearity was not observed in our experiments. Therefore, it can be assumed that in the experiments, the slippage of the collagen fibril on the supporting PDMS surface can be ignored in the calculation of the Young's modulus.

CONCLUSIONS

In the present study, we developed a method and determined the mechanical properties of single collagen fibrils by bending tests using AFM. PDMS substrates with a micro-channel structure could be well used to support single collagen fibrils. Fibrils spanning multiple PDMS channels were subjected to bending tests using an AFM cantilever without a tip. From the deflection-piezo displacement curve, force-indentation curves could be deduced and with the assumption that the deformation of collagen fibrils follows the linear elastic theory of isotropic materials, a Young's modulus of 5.4 GPa was calculated. After cross-linking with glutaraldehyde, the Young's modulus of a single fibril increases to 14.7 GPa. Because glutaraldehyde cross-linking enables binding of amine groups of (hydroxy)-lysine residues over distances of at least 1.3 nm it can be estimated that crosslinks are generated between collagen molecules as well as microfibrils. Further investigations will focus on single collagen fibrils cross-linked with different types of cross-linking agents to study the relationship between mechanical properties and collagen structure, also in an aqueous environment.

References

1. Silver FH, Freeman JW, Seehra GP. Collagen self-assembly and the development of tendon mechanical properties. J Biomech 2003;36:1529–1553.
2. Fratzl P, Misof K, Zizak I, Rapp G, Amenitsch H, Bernstorff S. Fibrillar structure and mechanical properties of collagen. J Struct Biol 1997;122:119–122.
3. Silver FH, Freeman JW, Horvath I, Landis WJ. Molecular basis for elastic energy storage in mineralized tendon. Biomacromolecules 2001;2:750–756.
4. Redaelli A, Vesentini S, Soncini M, Vena P, Mantero S, Montevecchi FM. Possible role of decorin glycosaminoglycans in fibril to fibril force transfer in relative mature tendons—A computational study from molecular to microstructural level. J Biomech 2003;36:1555–1569.
5. Scott JE. Extracelluar-matrix, supramolecular organization and shape. J Anat 1995;187:259–269.
6. Ottani V, Martini D, Franchi M, Ruggeri A, Raspanti M. Hierarchical structures in fibrillar collagens. Micron 2002;33:587–596.
7. Hulmes DJS. Building collagen molecules, fibrils, and suprafibrillar structures. J Struct Biol 2002;137:2–10.
8. Wess TJ, Hammersley AP, Wess L, Miller A. Molecular packing of type I collagen in tendon. J Mol Biol 1998;275:255–267.
9. Prockop DJ, Fertala A. The collagen fibril: The almost crystalline structure. J Struct Biol 1998;122:111–118.
10. Orgel JP, Miller A, Irving TC, Fischetti RF, Hammersley AP, Wess TJ. The in situ supermolecular structure of type I collagen. Structure 2001;9:1061–1069.
11. Holmes DF, Gilpin CJ, Baldock C, Ziese U, Koster AJ, Kadler KE. Corneal collagen fibril structure in three dimensions: Structural insights into fibril assembly, mechanical properties, and tissue organization. Proc Natl Acad Sci USA 2001;98:7307–7312.
12. Habelitz S, Balooch M, Marshall SJ, Balooch G, Marshall GW. In situ atomic force microscopy of partially demineralized human dentin collagen fibrils. J Struct Biol 2002;138:227–236.
13. Baselt D, Revel J, Baldeschwieler J. Subfibrillar structure of type I collagen observed by atomic force microscopy. Biophys J 1993;65:2644–2655.
14. An K, Sun Y, Luo Z. Flexibility of type I collagen and mechanical property of connective tissue. Biorheology 2004;41: 239–246.
15. Takaku K, Ogawa T, Kuriyama T, Narisawa I. Fracture behavior and morphology of spun collagen fibers. J Appl Polym Sci 1996;59:887–896.
16. Pins GD, Silver FH. A self-assembled collagen scaffold suitable for use in soft and hard tissue replacement. Mater Sci Eng C 1995;3:101–107.
17. Silver FH, Christiansen D, Snowhill PB, Chen Y, Landis WJ. The role of mineral in the storage of elastic energy in turkey tendons. Biomacromolecules 2000;1:180–185.
18. Puxkandl R, Zizak I, Paris O, Keckes J, Tesch W, Bernstorff S, Purslow P, Fratzl P. Viscoelastic properties of collagen: Synchrotron radiation investigations and structural model. Phil Trans R Soc Lond B Biol Sci 2002;357:191–197.
19. Sasaki N, Odajima S. Elongation mechanism of collagen fibrils and force-strain relations of tendon at each level of structural hierarchy. J Biomech 1996;29:1131–1136.
20. Sasaki N, Odajima S. Stress-strain curve and young's modulus of a collagen molecule as determined by the x-ray diffraction technique. J Biomech 1996;29:655–658.
21. Thompson JB, Kindt JH, Drake B, Hansma HG, Morse DE, Hansma PK. Bone indentation recovery time correlates with bond reforming time. Nature 2001;414:773–776.
22. Wang X, Li X, Yost M. Microtensile testing of collagen fibril for cardiovascular tissue engineering. J Biomed Mater Res A 2005;74:263–268.
23. Gutsmann T, Fantner GE, Kindt JH, Venturoni M, Danielsen S, Hansma PK. Force spectroscopy of collagen fibers to investigate their mechanical properties and structural organization. Biophys J 2004;86:3186–3193.
24. Graham JS, Vomund AN, Phillips CL, Grandbois M. Structural changes in human type I collagen fibrils investigated by force spectroscopy. Exp Cell Res 2004;299:335–342.
25. Bozec L, Horton M. Topography and mechanical properties of single molecules of type I collagen using atomic force microscopy. Biophys J 2005;88:4223–4231.
26. Venturoni M, Gutsmann T, Fantner GE, Kindt JH, Hansma PK. Investigations into the polymorphism of rat tail tendon fibrils using atomic force microscopy. Biochem Biophys Res Commun 2003;303:508–513.
27. Sun Y, Luo Z, Fertala A, An K. Direct quantification of the flexibility of type I collagen monomer. Biochem Biophys Res Commun 2002;295:382–386.
28. Namazu T, Isono Y, Tanaka T. Evaluation of size effect on mechanical properties of single crystal silicon by nanoscale bending test using AFM. J Microelectromech Syst 2000;9:450–459.

29. Salvetat J-P, Briggs G, Bonard J-M, Bacsa R, Kulik A, Stöckli T, Burnham N, Forró L. Elastic and shear moduli of single-walled carbon nanotube ropes. Phys Rev Lett 1999;82:944–947.
30. Gratzer PF, Lee JM. Altered mechanical properties in aortic elastic tissue using glutaraldehyde/solvent solutions of various dielectric constant. J Biomed Mater Res A 1997;37:497–507.
31. Olde Damink LHH, Dijkstra PJ, van Luyn MJA, van Wachem PB, Nieuwenhuis P, Feijen J. Glutaraldehyde as a crosslinking agent for collagen-based biomaterials. J Mater Sci: Mater Med 1995;6:460–472.
32. Friess W, Lee G. Basic thermoanalytical studies of insoluble collagen matrices. Biomaterials 1996;17:2289–2294.
33. Torii A, Sasaki M, Hane K, Okuma S. A method for determining the spring constant of cantilevers for atomic force microscopy. Meas Sci Technol 1996;7:179–184.
34. Serre C, Pérez-Rodrýguez A, Morante JR, Gorostiza P, Esteve J. Determination of micromechanical properties of thin films by beam bending measurements with an atomic force microscope. Sens Actuators 1999;74:134–138.
35. Gere J, Timoshenko S. Mechanics of Materials. Cheltenham, UK: Stanley Thornes; 1999. pp 511–700.
36. Silver FH, Christiansen DL, Snowhill PB, Chen Y. Transition from viscous to elastic-based dependency of mechanical properties of self-assembled type I collagen fibers. J Appl Polym Sci 2001;79:134–142.
37. Mele E, Benedetto F, Persano L, Pisignano D, Cingolani R. Combined capillary force and step and flash lithography. Nanotechnology 2005;16:391–395.
38. Ljungcrantz H, Hultman L, Sundgren J, Johansson S, Kristensen N, Schweitz J. Residual stresses and fracture properties of magnetron sputtered Ti films on Si microelements. J Vac Sci Technol A 1993;11:543–553.